Inorg. Chem. **2007**, *46*, 10850–10859

Inorganic Chemistry
Article

Mechanism of the MoO_2Cl_2-Catalyzed Hydrosilylation: A DFT Study

Markus Drees and Thomas Strassner*

Technische Universitaet Dresden, Professur fuer Physikalische Organische Chemie, Bergstr. 66, D-01062 Dresden, Germany

Received September 3, 2007

A detailed mechanistic study of the hydrosilylation of benzaldehyde catalyzed by MoO_2Cl_2 is reported. On the basis of DFT calculations (B3LYP/6-311++G**), a reaction pathway via initial silane activation is proposed. SiH and CH activation energies by other metal-oxo compounds like RuO_4, OsO_4, and MnO_4^- are compared to MoO_2Cl_2. MO_4-type metal-oxo compounds follow a different mechanism, forming highly exergonic intermediates, which prevent a catalytic reaction, whereas MoO_2Cl_2 prefers a reaction pathway via thermoneutral intermediates.

Introduction

The hydrosilylation reaction is a very convenient and important way of introducing silylated groups into organic compounds. Organosilicon compounds are used in large quantities and are of industrial importance. There are many applications known, for example, in polymer chemistry.[1−3] It is well-known that transition metals like platinum(0) are able to catalyze the addition of silanes to alkenes and are effective in creating carbon−silicon and silicon−oxygen bonds.[4−6]

However, quite recently an unconventional catalytic activity of high-valent metal-oxo compounds like $ReO_2I(PPh_3)_2$,[7] $ReO(hoz)_2$,[8] or MoO_2Cl_2[9,10] in the hydrosilylation of aldehydes and ketones was reported in the literature.[11−18]

Scheme 1. Catalytic Hydrosilylation as Reported by Romao et al[9]

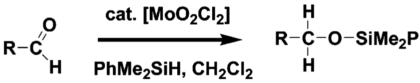

Scheme 2. Metal-oxo (MO_2X_2)-Catalyzed Hydrosilylation of Carbonyl Compounds via Initial SiH Activation

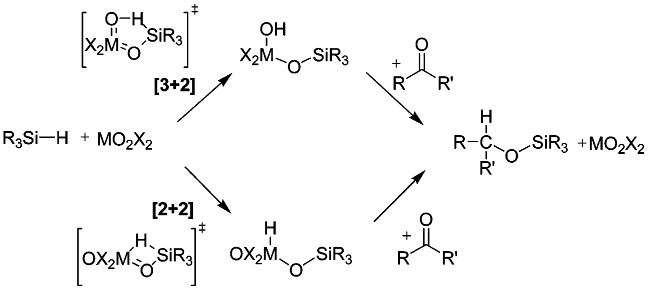

Especially in the case of MoO_2Cl_2, it was reported by Romao et al.[9,10] that this compound effectively catalyzes the hydrosilylation of aromatic aldehydes and ketones (Scheme 1).

Different mechanisms have been proposed along with experimental studies for the different metal-oxo agents.[7−10,19,20]

---

* To whom correspondence should be addressed. E-mail: thomas.strassner@chemie.tu-dresden.de.

(1) Ojima, I. In *The Chemistry of Organosilicon Compounds*; Patai, S., Rappoport, Z., Eds.; John Wiley and Sons: New York, 1989; p 1479.
(2) Ojima, I.; Li, Z.; Zhu, J. In *The Chemistry of Organosilicon Compounds*; Rappoport, Z., Apeloig, Y., Eds.; Wiley and Sons: New York, 1998; p 1687.
(3) Hiyama, T.; Kusumoto, T. In *Comprehensive Organic Synthesis*; Trost, B. M., Fleming, I., Eds.; Pergamon Press: Oxford, 1991; Vol. 8, p 763.
(4) Trost, B. M. *Science* **1991**, *254*, 1471−7.
(5) Trost, B. M. *Acc. Chem. Res.* **2002**, *35*, 695−705.
(6) Trost, B. M. *Angew. Chem., Int. Ed. Engl.* **1995**, *34*, 259−81.
(7) Kennedy-Smith, J. J.; Nolin, K. A.; Gunterman, H. P.; Toste, F. D. *J. Am. Chem. Soc.* **2003**, *125*, 4056−4057.
(8) Ison, E. A.; Trivedi, E. R.; Corbin, R. A.; Abu-Omar, M. M. *J. Am. Chem. Soc.* **2005**, *127*, 15374−15375.
(9) Fernandes, A. C.; Fernandes, R.; Romao, C. C.; Royo, B. *Chem. Commun.* **2005**, 213−214.
(10) Reis, P. M.; Romao, C. C.; Royo, B. *Dalton Trans.* **2006**, 1842−1846.
(11) Ison, E. A.; Cessarich, J. E.; Du, G.; Fanwick, P. E.; Abu-Omar, M. M. *Inorg. Chem.* **2006**, *45*, 2385−2387.
(12) Trost, B. M.; Fleming, I. *Comprehensive Organic Synthesis*; Pergamon Press: Oxford, U.K., 1991; Vol. 7.
(13) Burke, S. D.; Danheiser, R. L. *Handbook of Reagents for Organic Synthesis: Oxidizing and Reducing Agents*; Wiley and Sons: New York, 1999.
(14) Nugent, W. A.; Mayer, J. M. *Metal-Ligand Multiple Bonds*; Wiley and Sons: New York, 1988.
(15) Romao, C. C.; Kuehn, F. E.; Herrmann, W. A. *Chem. Rev.* **1997**, *97*, 3197−3246.
(16) Owens, G. S.; Arias, J.; Abu-Omar, M. M. *Catal. Today* **2000**, *55*, 317−363.
(17) Gable, K. P. *Adv. Organomet. Chem.* **1997**, *41*, 127−161.
(18) Holm, R. H. *Chem. Rev.* **1987**, *87*, 1401−49.
(19) Du, G.; Fanwick, P. E.; Abu-Omar, M. M. *J. Am. Chem. Soc.*, **2007**, *129*, 5180−5187.
(20) Valliant-Saunders, K.; Gunn, E.; Shelton, G. R.; Hrovat, D. A.; Borden, W. T.; Mayer, J. M. *Inorg. Chem.* **2007**, *46*, 5212−5219.

10.1021/ic7017314 CCC: $37.00

Scheme 3. Possible Reaction Pathways for the MoO_2Cl_2-Catalyzed Hydrosilylation via Initial Silane Activation (Blue = Feasible Pathway According to This Study)

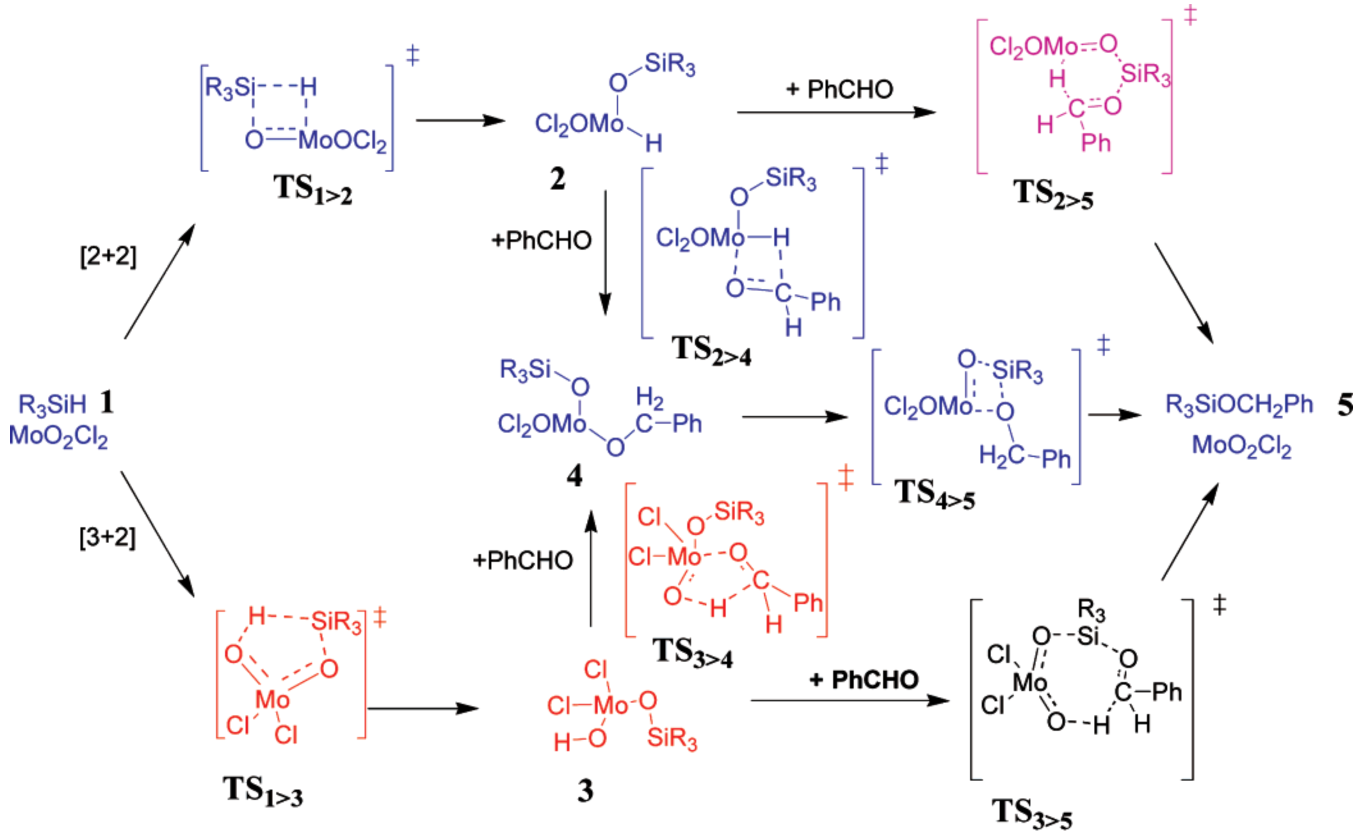

Table 1. Activation Barriers and Relative Energies of Intermediates for the Oxidative Addition of SiH_4 and CH_4 to Different Metal-oxo Compounds (in kcal/mol; B3LYP/6-311++G**; bold = Preferred Pathway)

SiH_4	transition state		intermediate		transition state		intermediate	
	$\Delta H^\ddagger(2+2)$	$\Delta G^\ddagger(2+2)$	$\Delta H_i\,(2+2)$	$\Delta G_i\,(2+2)$	$\Delta H^\ddagger\,(3+2)$	$\Delta G^\ddagger\,(3+2)$	$\Delta H_i\,(3+2)$	$\Delta G_i\,(3+2)$
MoO_2Cl_2	**+25.8**	**+35.8**	**−7.2**	**+1.0**	+36.9	+46.7	−3.0	+3.9
MnO_4^-	+28.5	+37.5	+8.1	+15.3	**+2.6**	**+11.3**	**−68.5**	**−62.0**
RuO_4	+39.3	+48.0	−1.4	+5.5	**+ 5.3**	**+13.5**	**−70.2**	**−63.2**
OsO_4	+37.6	+46.1	−3.0	+4.2	**+11.9**	**+20.4**	**−47.3**	**−40.5**
CH_4	transition state		intermediate		transition state		intermediate	
	$\Delta H^\ddagger\,(2+2)$	$\Delta G^\ddagger\,(2+2)$	$\Delta H_i\,(2+2)$	$\Delta G_i\,(2+2)$	$\Delta H^\ddagger\,(3+2)$	$\Delta G^\ddagger\,(3+2)$	$\Delta H_i\,(3+2)$	$\Delta G_i\,(3+2)$
MoO_2Cl_2	+88.5	+97.0	**+31.6**	**+39.7**	**+70.8**	**+79.0**	+36.2	+43.9
MnO_4^-	N/A[a]	N/A[a]	+53.3	+60.8	**+33.8**	**+38.6**	**−20.2**	**−13.2**
RuO_4	+108.7	+116.0	+34.3	+42.1	**+22.6**	**+30.9**	**−34.1**	**−26.4**
OsO_4	+110.1	+117.5	+33.4	+41.4	**+33.6**	**+41.9**	**−10.2**	**- 2.7**

[a] Every transition state search lead to the [3+2] transition state, which is an indication for an even higher energy of the missing [2+2] transition state.

The most prominent one is a [2+2] cycloaddition of the silane to a hydride intermediate, followed by the addition of the carbonyl substrate. However, as known from the CH activation by metal-oxo compounds, a [3+2] pathway via a hydroxide intermediate might be possible as well. For the catalysis observed by Toste et al. ,[7] a thorough DFT study by Wu et al.[21] concluded that the hydrosilylation at $ReO_2I(PPh_3)_2$ indeed proceeds via an initial [2+2] mechanism. A metathesis-like mechanism was initially proposed for the $ReO_2(hoz)_2$ and $ReO(L)(hoz)_2$ complexes,[8] but it was later shown to be unfavorable.[21] A quite recent article on the molybdenum system by Calhorda et al. took into account different mechanisms including solvent effects but did not include the experimentally used silanes. Using model silanes like SiH_4 and $HSiMe_3$, they could not distinguish between the different possible pathways (including radical pathways) on the double-ξ level of theory.[22]

We are generally interested in the catalytic activity of metal-oxo compounds and have already investigated the activation of CH bonds by related metal-oxo compounds like permanganate[23] or ruthenium tetraoxide[24] and continued our work also in the area of SiH activation by d^0 metal-oxo compounds, comparing the [2+2] and [3+2] reaction pathways for RuO_4, OsO_4, MnO_4^-, and MoO_2Cl_2 in the oxidation of SiH_4 and CH_4 (Scheme 2).

---

(21) Chung, L. W.; Lee, H. G.; Lin, Z.; Wu, Y.-D. *J. Org. Chem.* **2006**, *71*, 6000−6009.

(22) Costa, P. J.; Romao, C. C.; Fernandes, A. C.; Royo, B.; Reis, P. M.; Calhorda, M. J. *Chem.*—*Eur. J.* **2007**, *13*, 3934−3941.

(23) Strassner, T.; Houk, K. N. *J. Am. Chem. Soc.* **2000**, *122*, 7821−7822.

(24) Drees, M.; Strassner, T. *J. Org. Chem.* **2006**, *71*, 1755−1760.

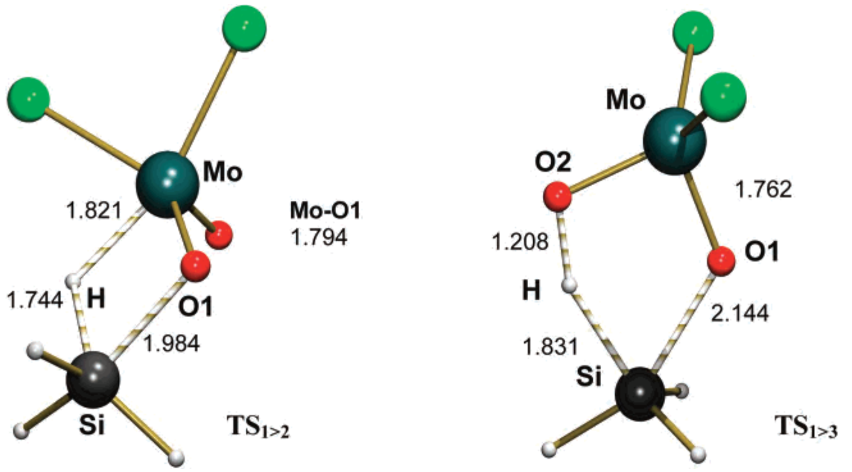

Figure 1. Transition states $\mathbf{TS_{1>2}}$ ([2+2] pathway) and $\mathbf{TS_{1>3}}$ ([3+2] pathway), bond lengths in angstroms.

Scheme 4. Free-Energy Plot of the Possible Pathways for the Catalytic Hydrosilylation of Benzaldehyde with SiH_4 − Initial Silane Activation (Blue = Most Feasible, All Energies Relative to the Starting Materials)

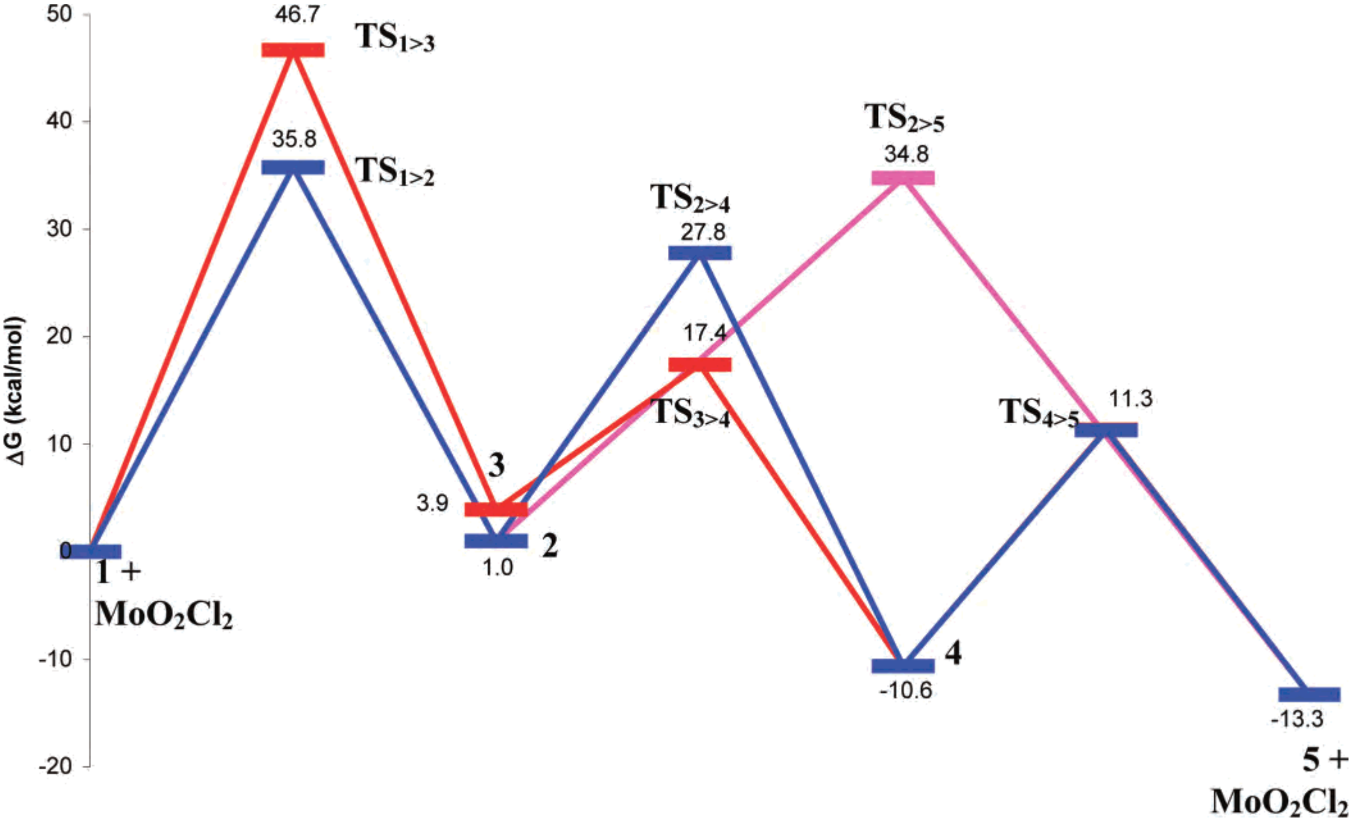

For the molybdenum catalyst, an initial [2+2] addition of the silane to the molybdenum catalyst is postulated,[9,10] but the role of the carbonyl compound remained unclear.[22] On the basis of triple-ξ DFT calculations (B3LYP/6-311++G**), we present a detailed study of the different pathways for this hydrosilylation reaction. We analyze the role of both reactants and their interaction with the catalyst, distinguishing between the initial addition of the carbonyl compound *or* the silane in the system $MoO_2Cl_2/SiH_4/PhCHO$. We also calculated the preferred pathway for the experimentally used dimethylphenylsilane ($PhMe_2SiH$). For comparison, we also calculated the uncatalyzed hydrosilylation of bezaldehyde by SiH_4 or Me_2PhSiH, which was found to proceed via a very high barrier of around 55 kcal/mol ($\Delta G^{\neq}$) for both silanes, which explains the need for a catalyst for this reaction. We also compare our study to the work of Wu et al.[21] and their results for $ReO_2I(PPh_3)_2$ as the molecular catalyst as well as our triple-ξ results to those on the double-ξ level of theory,[22] at the end of the results and discussion section.

Computational Details. All of the calculations were performed with *Gaussian 03*[25] using the density-functional/Hartree−Fock hybrid model Becke3LYP[26−29] and the split valence triple-ζ (TZ) basis set 6-311++G**[30,31] for carbon, hydrogen, oxygen, silicon, and manganese. The Stuttgart/Dresden 1997 ECP[32] was used for molybdenum, ruthenium,

Scheme 5. Competing Pathways via Initial Carbonyl Activation at the MoO_2Cl_2 Catalyst (Blue = Most-Feasible Pathway for the Initial Carbonyl Coordination)

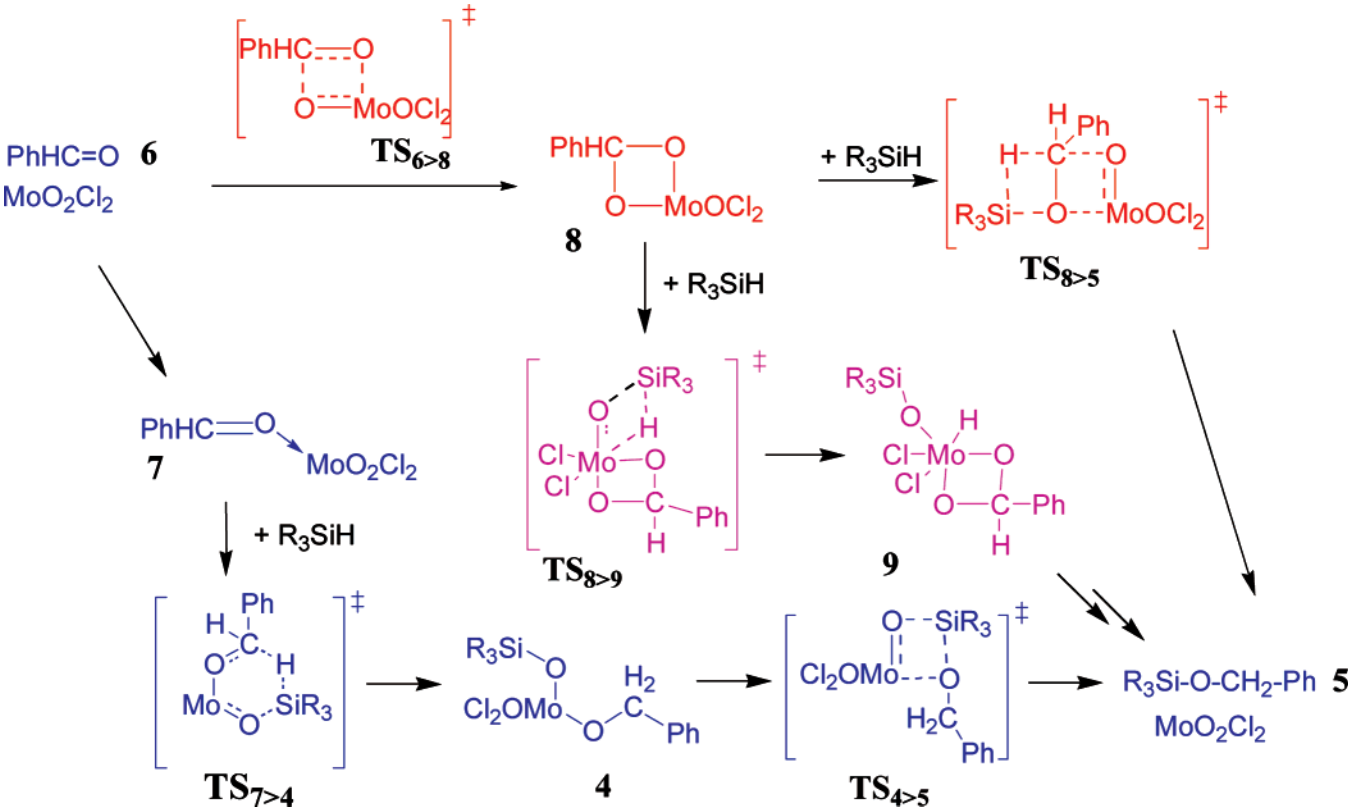

Table 2. Relative Enthalpies, Free Energies, and QCISD(T) Energies (in kcal/mol) for the MoO_2Cl_2-Catalyzed Hydrosilylation of PhCHO with SiH_4 via Initial SiH Activation at MoO_2Cl_2 (Blue = Preferred Mechanism; All Energies Are Given Relative to the Starting Materials)

	$TS_{1>2}$	2	$TS_{1>3}$	3	$TS_{2>4}$	$TS_{3>4}$	4	$TS_{4>5}$	$TS_{2>5}$	products[a]
ΔH[b]	**25.8**	**−7.2**	36.8	−3.0	**5.8**	−4.0	**−30.6**	**−11.8**	11.6	**−21.7**
ΔG[b]	**35.8**	**1.0**	46.7	3.9	**27.8**	17.4	**−10.6**	**11.3**	34.8	**−13.3**
ΔE[c]	**21.6**	**−5.7**	40.4	11.9						

[a] $PhCH_2OSiH_3$ (**5**) + MoO_2Cl_2. [b] B3LYP/6-311++G**. [c] QCISD(T)/6-311++G**//B3LYP/6-311++G**.

and osmium. No symmetry or internal coordinate constraints were applied during optimizations. Where possible, QCISD(T)[33] energy calculations were run on the DFT-optimized structures (QCISD(T)/6-311++G**// B3LYP/6-311++G**). All of the reported intermediates were verified as true minima by the absence of negative eigenvalues in the vibrational frequency analysis. Transition-state structures (indicated by TS) were located using the Berny algorithm[34] until the Hessian matrix had only one imaginary eigenvalue. The identity of all of the transition states was confirmed by IRC calculations and by animating the negative eigenvector coordinate with *MOLDEN*[35] and *GaussView*.[36]

Approximate free energies (ΔG) and enthalpies (ΔH) were obtained through thermochemical analysis of frequency calculations, using the thermal correction to Gibbs free energy as reported by *Gaussian 03*. This takes into account zero-point effects, thermal enthalpy corrections, and entropy.

---

(25) Frisch, M. J.; Trucks, G. W.; Schlegel, H. B.; Scuseria, G. E.; Robb, M. A.; Cheeseman, J. R.; Montgomery, J. A., Jr.; Vreven, T.; Kudin, K. N.; Burant, J. C.; Millam, J. M.; Iyengar, S. S.; Tomasi, J.; Barone, V.; Mennucci, B.; Cossi, M.; Scalmani, G.; Rega, N.; Petersson, G. A.; Nakatsuji, H.; Hada, M.; Ehara, M.; Toyota, K.; Fukuda, R.; Hasegawa, J.; Ishida, M.; Nakajima, T.; Honda, Y.; Kitao, O.; Nakai, H.; Klene, M.; Li, X.; Knox, J. E.; Hratchian, H. P.; Cross, J. B.; Bakken, V.; Adamo, C.; Jaramillo, J.; Gomperts, R.; Stratmann, R. E.; Yazyev, O.; Austin, A. J.; Cammi, R.; Pomelli, C.; Ochterski, J. W.; Ayala, P. Y.; Morokuma, K.; Voth, G. A.; Salvador, P.; Dannenberg, J. J.; Zakrzewski, V. G.; Dapprich, S.; Daniels, A. D.; Strain, M. C.; Farkas, O.; Malick, D. K.; Rabuck, A. D.; Raghavachari, K.; Foresman, J. B.; Ortiz, J. V.; Cui, Q.; Baboul, A. G.; Clifford, S.; Cioslowski, J.; Stefanov, B. B.; Liu, G.; Liashenko, A.; Piskorz, P.; Komaromi, I.; Martin, R. L.; Fox, D. J.; Keith, T.; Al-Laham, M. A.; Peng, C. Y.; Nanayakkara, A.; Challacombe, M.; Gill, P. M. W.; Johnson, B.; Chen, W.; Wong, M. W.; Gonzalez, C.; Pople, J. A. *Gaussian 03*, revision C.02; Gaussian, Inc.: Wallingford, CT, 2004.

(26) Lee, C. Y., W.; Parr, R. G. *Phys. Rev. B* **1988**, *37*, 785−789.

(27) Vosko, S. H. W. L.; Nusair, M. *Can. J. Phys.* **1980**, *58*, 1200−1211.

(28) Becke, A. D. *J. Chem. Phys.* **1993**, *98*, 5648−5652.

(29) Stephens, P. J. D., F. J.; Chabalowski, C. F.; Frisch, M. J. *J. Phys. Chem.* **1994**, *98*, 11623−11627.

(30) Krishnan, R.; Binkley, J. S.; Seeger, R.; Pople, J. A. *J. Chem. Phys.* **1980**, *72*, 650−4.

(31) Clark, T.; Chandrasekhar, J.; Spitznagel, G. W.; Schleyer, P. v. R. *J. Comput. Chem.* **1983**, *4*, 294−301.

(32) Andrae, D.; Haeussermann, U.; Dolg, M.; Stoll, H.; Preuss, H. *Theor. Chim. Acta* **1990**, *77*, 123−41.

(33) Pople, J. A.; Head-Gordon, M.; Raghavachari, K. *J. Chem. Phys.* **1987**, *87*, 5968−75.

(34) Schlegel, H. B. *J. Comput. Chem.* **1982**, *3*, 214−218.

(35) Schaftenaar, G.; Noordik, J. H. *J. Comput.-Aided Mol. Design* **2000**, *14*, 123−134.

(36) Dennington II, R.; Keith, T.; Millam, J.; Eppinnett, K.; Hovell, W. L.; Gilliland, R. *GaussView 3.09*; Semichem, Inc.: Shawnee Mission, KS, 2003.

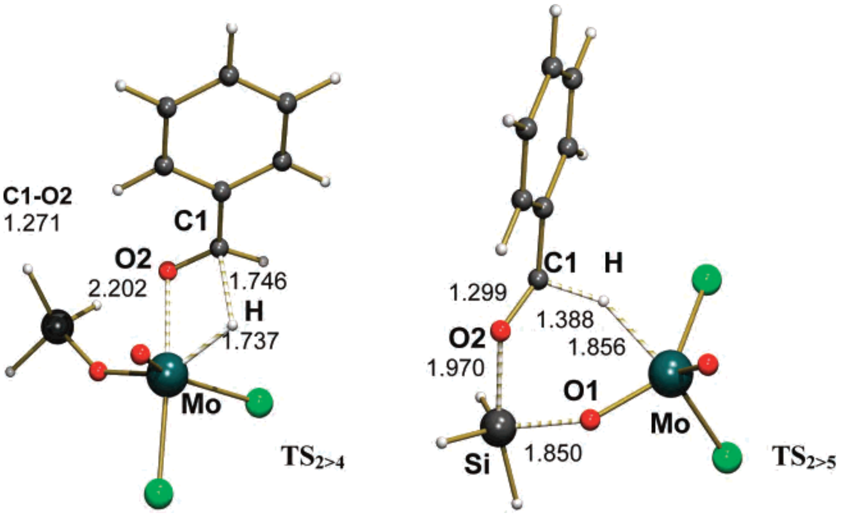

Figure 2. Transition state $\mathbf{TS}_{2>4}$ (stepwise mechanism) and $\mathbf{TS}_{2>5}$ (concerted mechanism), bond lengths in angstroms.

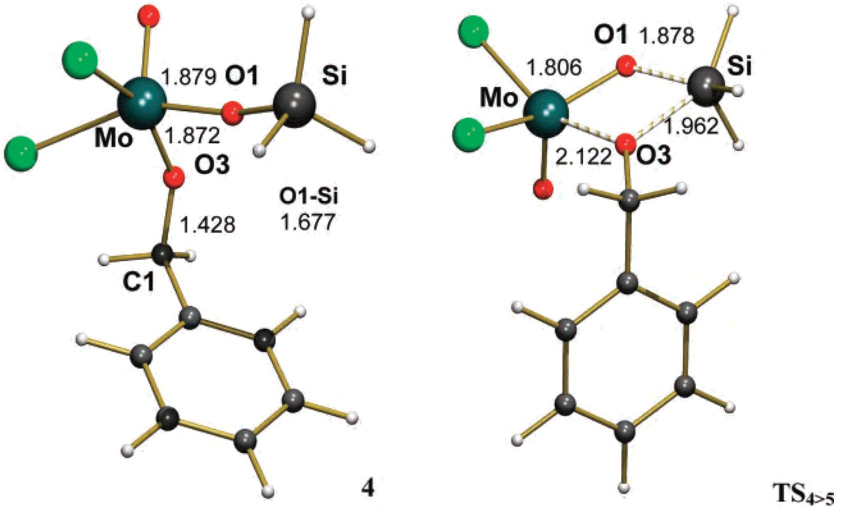

Figure 3. Intermediate **4** and transition state $\mathbf{TS}_{4>5}$, bond lengths in angstroms.

Table 3. Relative Enthalpies and Free Energies (B3LYP/6-311++G**, in kcal/mol) for the Hydrosilylation of PhCHO with SiH_4 via Initial Carbonyl Activation at MoO_2Cl_2 (Blue = Preferred Mechanism; All Energies Are Given Relative to the Starting Materials)

	7	$TS_{7>4}$	$TS_{6>8}$	8	$TS_{8>5}$	$TS_{8>9}$	9	products[a]
ΔH^a	−7.3	16.1	20.1	13.3	30.6	41.1	10.9	−21.7
ΔG^a	3.7	38.4	32.8	25.8	52.3	64.2	32.5	−13.3

[a] $PhCH_2OSiH_3$ (**5**) + MoO_2Cl_2.

All of the energies reported in this article, unless otherwise noted, are free energies or enthalpies at 298 K, using unscaled frequencies. The results are discussed in the light of a recent article on the QM assessment of catalytic cycles.[37] All of the transition states are maxima on the electronic potential energy surface, which may not correspond to maxima on the free-energy surface.

Results and Discussion

As mentioned above, all of the previously postulated mechanisms propose an initial SiH activation. In analogy to the CH activation, two different reaction pathways are possible. The activation of the SiH bond can be accomplished at the metal center and one of the oxygens in a [2+2] reaction or via two oxygens ([3+2] reaction). The carbonyl compound then reacts with the corresponding intermediate (Scheme 2).

To compare barriers for the SiH and CH activation, we first studied the reaction of CH_4 and SiH_4 with MoO_2Cl_2 and compared the results to the calculated activation energies of other metal-oxo compounds (OsO_4, RuO_4, and MnO_4^-). The energies for the [2+2] and [3+2] transition states and intermediates for SiH_4 and CH_4 are summarized in Table 1.

The results given in Table 1 show that for the MO_4 agents the [3+2] reaction pathway is the preferred mechanism for the CH and for the SiH activation reactions, in agreement with a recent article on the oxidation of silanes by OsO_4.[20] The calculated free-energy differences between the [2+2] and the [3+2] transition state are smaller for the oxidation of SiH_4 compared to the CH_4 oxidation, with a difference of up to 85 kcal/mol. Of course, the higher energies for the methane activation are in good agreement with the experimentally known inertness of methane in comparison to SiH_4.

In the case of MoO_2Cl_2, things are different. Here, the [2+2] mechanism is the preferred reaction pathway for the

---

(37) Kozuch, S.; Shaik, S. *J. Am. Chem. Soc.* **2006**, *128*, 3355−3365.

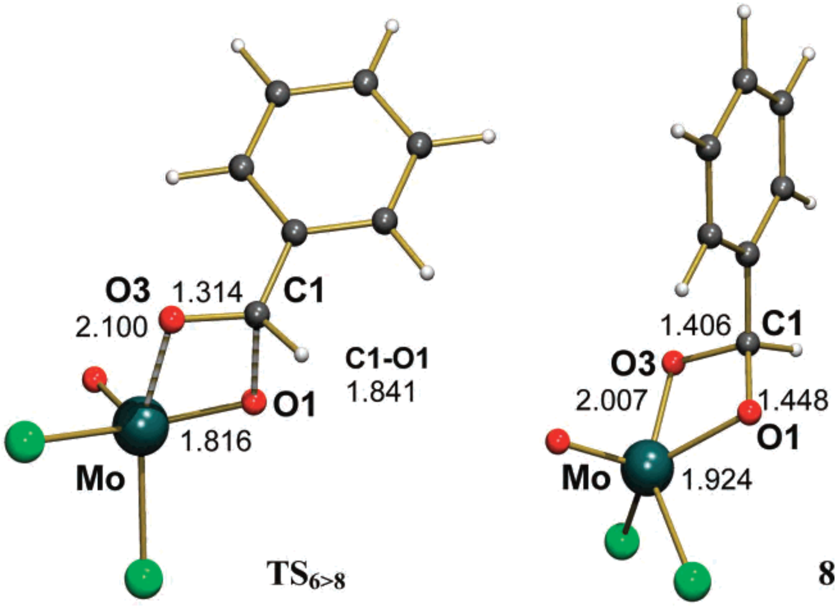

Figure 4. Transition state $\mathbf{TS_{6>8}}$ and subsequent intermediate **8**, atomic distances in angstroms.

Scheme 6. Free-Energy Plot of the Possible Pathways for the Catalytic Hydrosilylation of Benzaldehyde with SiH_4 − Initial Carbonyl Activation (Blue = Most Feasible, All Energies Relative to the Starting Materials)

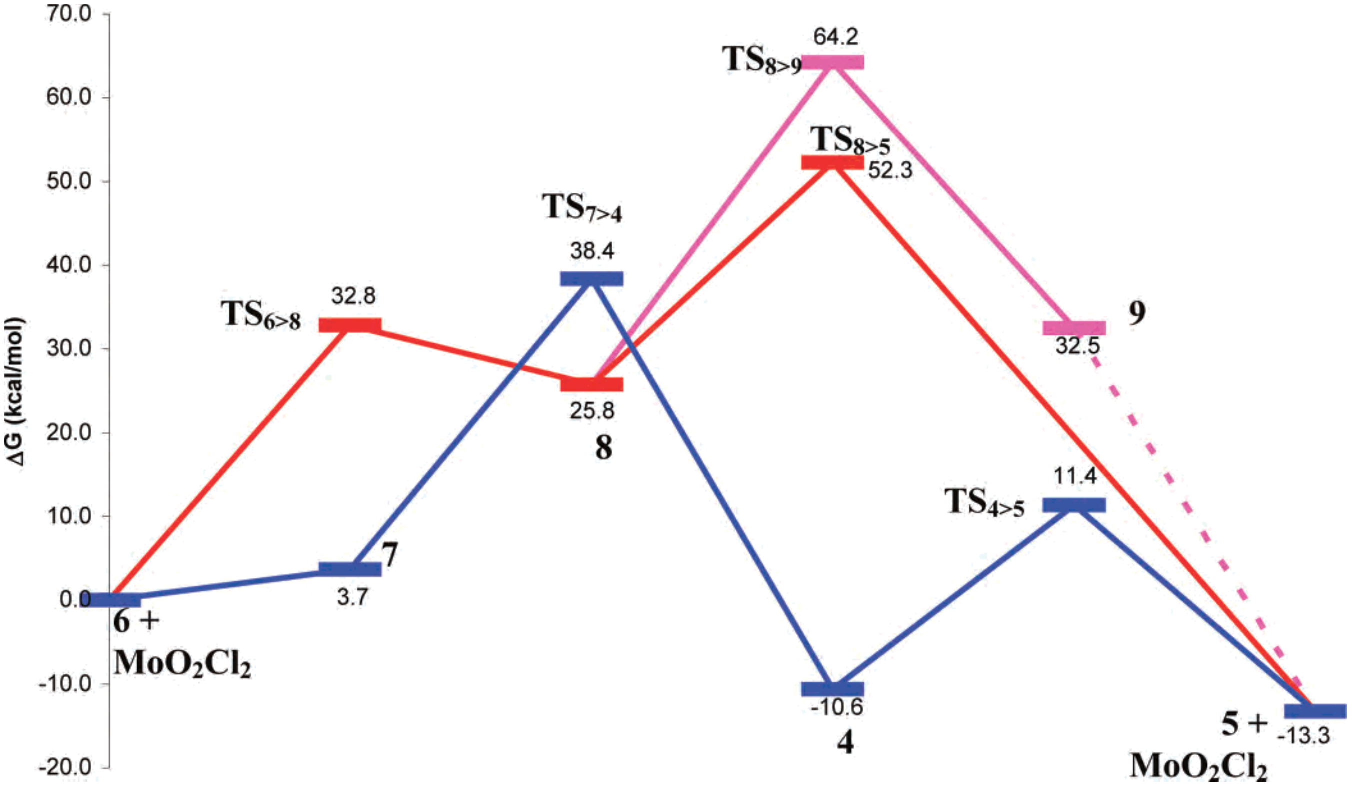

SiH activation, thermodynamically as well as kinetically. Its transition state is 10 kcal/mol lower in energy compared to the [3+2] activation barrier. The [2+2] hydride intermediate is also slightly less endergonic than the [3+2] molybdenum hydroxyl compound. Although both transition states are very high in energy, the CH activation mediated by MoO_2Cl_2 shows a kinetical preference for the [3+2] mechanism, whereas the comparison of the two intermediates reveals that the [2+2] hydride species is less endergonic by 4 kcal/mol.

The stability of the [3+2] intermediates of the SiH activation by MO_4 compounds prohibits a catalytic reaction as proposed in Scheme 2, whereas the calculated barriers and the energy of the [2+2] intermediate of the MoO_2Cl_2 oxidation are in good agreement with what would be expected for a catalytic reaction.

$SiH_4/MoO_2Cl_2 \Rightarrow C_6H_5CHO$

We therefore analyzed the MoO_2Cl_2-catalyzed hydrosilylation of benzaldehyde with initial SiH_4 (**1**) activation

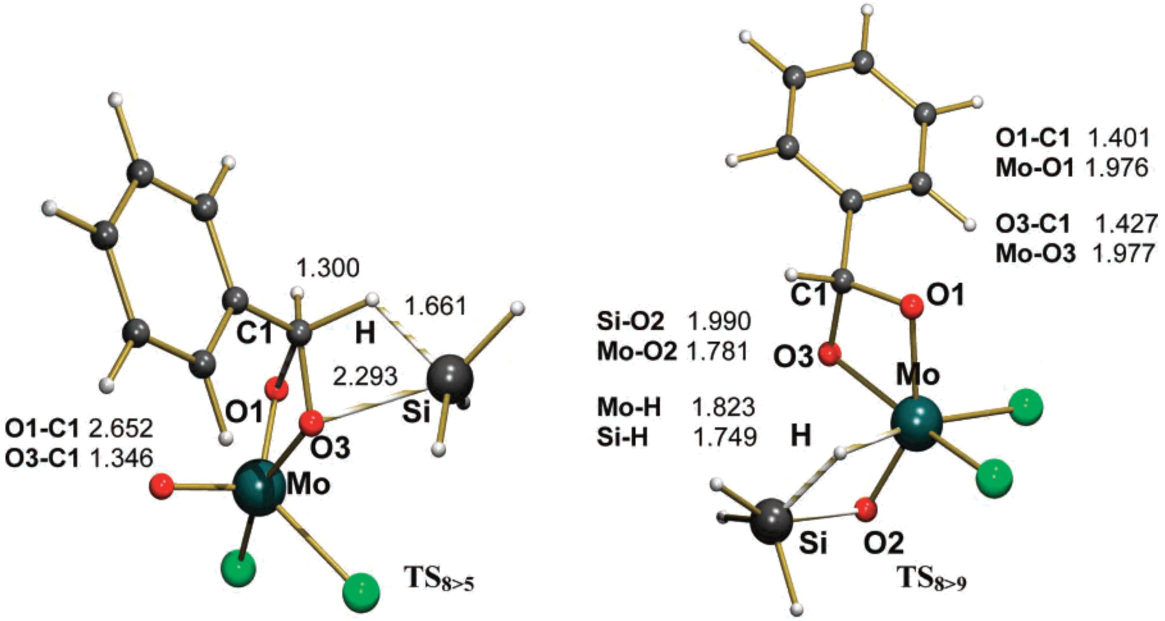

Figure 5. Transition state **TS$_{8>5}$** (concerted hydrosilylation) and **TS$_{8>9}$** (Si−H activation at Mo−O2), atomic distances in angstroms.

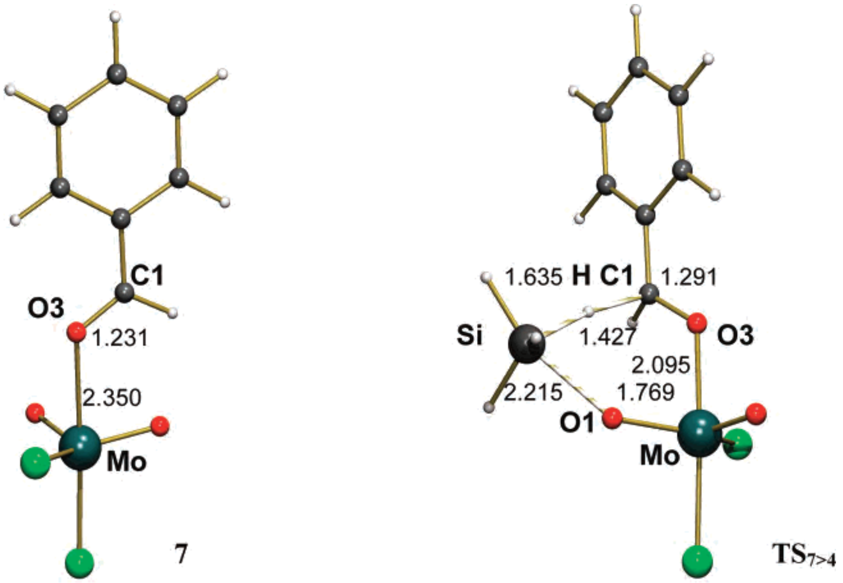

Figure 6. Benzaldehyde-MoO_2Cl_2 **7** and hydrosilylation transition state **TS$_{7>4}$**, atomic distances in angstroms.

(Scheme 3). Competing pathways via initial carbonyl coordination are discussed later (Scheme 5).

The [2+2] pathway via the four-membered cyclic transition state **TS$_{1>2}$** leads to the metal hydride adduct **2**. The alternative [3+2] mechanism via transition state **TS$_{1>3}$** produces the hydroxyl intermediate **3**. The formation of the hydrosilylation product **5** can proceed via different pathways. One is the concerted addition of the carbonyl compound via a six-membered (**TS$_{2>5}$**) or seven-membered transition state (**TS$_{3>5}$**) without coordination of the carbonyl group to the catalyst. An alternative mechanism requires the interaction of the carbonyl oxygen atom with the metal center. For both intermediates (**2** → **TS$_{2>4}$** and **3** → **TS$_{3>4}$**), this reaction step involves the transfer of the former silyl hydrogen to the carbonyl carbon, leading to the same intermediate **4**. Elimination of the hydrosilylation product **5** from the catalyst via **TS$_{4>5}$** is the final step of this reaction pathway.

The calculated energies for these pathways are given in Table 2, whereas a plot of the free energies is found in Scheme 4. Where possible, we added QCISD(T) single-point calculations to get the most accurate energies. The single-point energies confirm that the [2+2] mechanism is favored. The [3+2] and the [2+2] transition states (**TS$_{1>2}$** and **TS$_{1>3}$**) are plotted in Figure 1.

A possible tautomerisation between intermediates **2** and **3** has also been considered. However, from the calculated activation energies ($\Delta G^{\ddagger} = 34.0$ kcal/mol for B3LYP/6-311++G** relative to **2**) of this reaction, this hydrogen transfer can be ruled out because the competing transition states **TS$_{2>4}$** or **TS$_{3>4}$** are all lower in relative free energies (Table 2). Starting from intermediates **2** and **3**, the direct formation of the hydrosilylation product **5** occurs via cyclic transition states. The seven-membered cyclic transition state **TS$_{3>5}$** leading from intermediate **3** to the product could not

Scheme 7. Free-Energy Plot of the Possible Pathways for the Catalytic Hydrosilylation of Benzaldehyde with $PhMe_2SiH$ (B3LYP/6-311++G**)

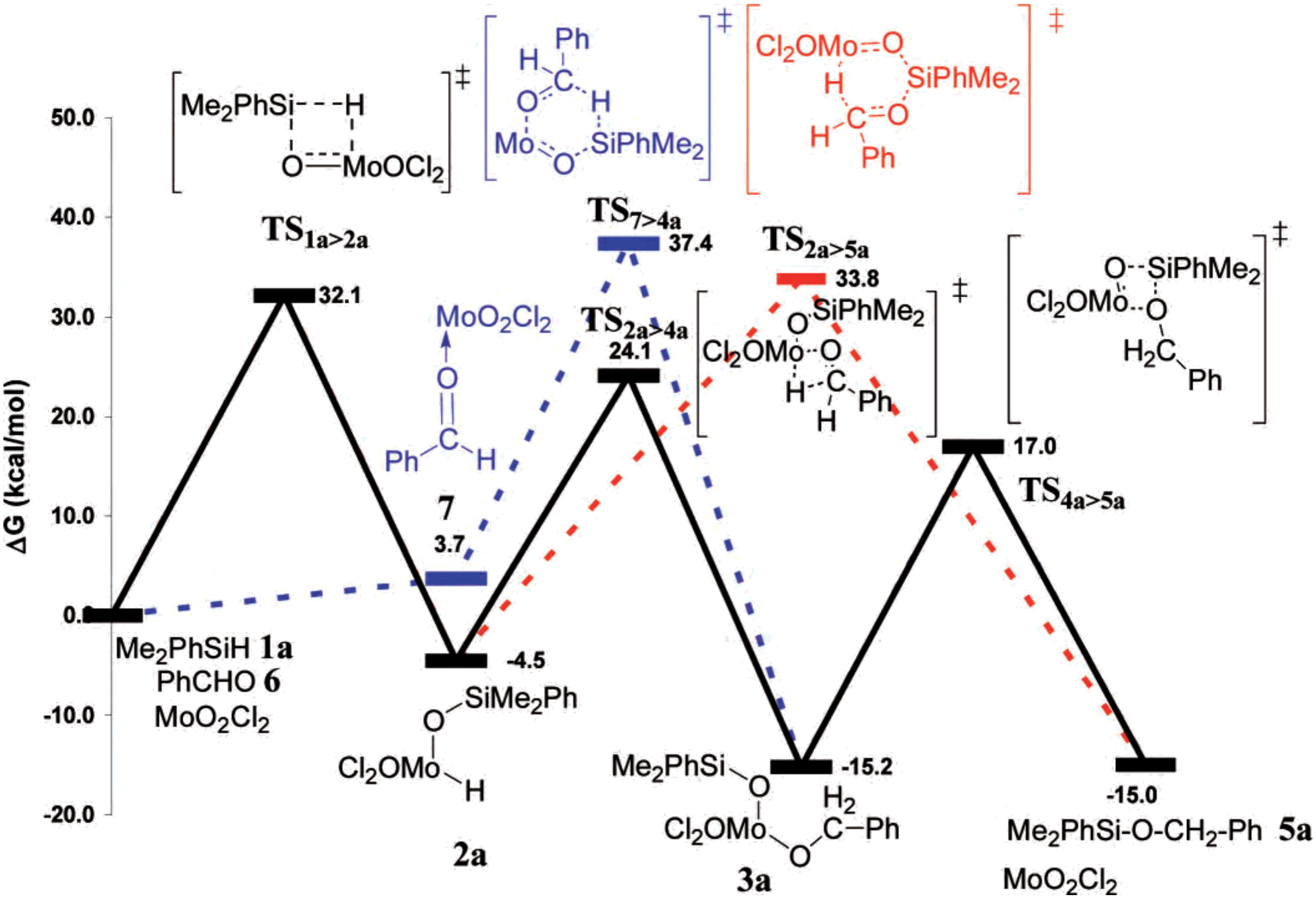

be localized on the energy hypersurface, although we got close enough to rule out that a pathway over the preceding transition state **TS**$_{1>3}$ and then **TS**$_{3>5}$ is not a reasonable pathway, according to our results.

The concerted reaction pathway via the intermediate hydride **2** with a barrier of 33.8 kcal/mol (**TS**$_{2>5}$, Figure 2) is higher in energy compared to a stepwise hydrosilylation pathway via intermediate **2** (**TS**$_{2>4}$, $\Delta G^{\ddagger}$(barrier) = 26.8 kcal/mol, Figure 2), which requires coordination of the carbonyl function.

Intermediate **4** (Figure 3, ΔG(rel) = −10.6 kcal/mol) is almost as exergonic as the final products (ΔG(rel) = −13.3 kcal/mol). Both Mo−O bonds (Mo−O1 and Mo−O3) can be considered single bonds with bond lengths of about 1.88 Å. The hydrosilylation carries on with the transfer of the silyl group from O1 to O3 via another four-membered ring in **TS**$_{4>5}$ (Figure 3, $\Delta G^{\ddagger}$(barrier) = 21.9 kcal/mol). By separating from the catalyst MoO_2Cl_2, the product $PhCH_2$-$OSiH_3$ is formed, completing the catalytic cycle.

$C_6H_5CHO/MoO_2Cl_2 \Rightarrow SiH_4$

Another possibility is the initial coordination of the carbonyl component (benzaldehyde **6**) to the metal-oxo catalyst, leading to different pathways for the hydrosilylation process (Scheme 5). We consider two different routes: formation of the simple adduct **7** or a [2+2] addition of the carbonyl C=O bond to one of the Mo=O double bonds (intermediate **8** via **TS**$_{6>8}$). From adduct **7**, the silane can be activated via a cyclic transition state **TS**$_{7>4}$ to form intermediate **4** (Figure 3). The four-membered cyclic intermediate **8** can react with the silane via two different concerted reaction pathways. A [2+2] addition at the former carbonyl bond (**TS**$_{8>5}$) directly leads to the hydrosilylation product **5**. Alternatively, the silane can also react with the remaining Mo−O double bond (**TS**$_{8>9}$) to form the molybdenum hydride species **9**.

Table 3 reports the energies of the relevant intermediates and transition states of the hydrosilylation pathways, starting with the coordination of the carbonyl compound to the catalyst (intermediate **4** and **TS**$_{4>5}$ are already given in Table 2). The plot in Scheme 6 illustrates the relative energies of all of the pathways starting with the coordination of the carbonyl group to the catalyst.

Although the formation of the endergonic intermediate **8** (ΔG(rel.) = +25.8 kcal/mol, Figure 4) only requires an activation energy of 32.8 kcal/mol via the [2+2] transition state **TS**$_{6>8}$ (Figure 4), the following transition states (**TS**$_{8>5}$ or **TS**$_{8>9}$, Figure 5), leading from **8** into both hydrosilylation pathways, require activation energies that are higher ($\Delta G^{\ddagger}$(barrier) = 26.5 kcal/mol, **TS**$_{8>5}$ // $\Delta G^{\ddagger}$(barrier) = 38.4 kcal/mol, **TS**$_{8>9}$) than the barrier for the cleavage of **8**, leading back to the starting materials ($\Delta G^{\ddagger}$(barrier) = 7.0

Scheme 8. Free-Energy Plot of the Possible Pathways for the Catalytic Hydrosilylation of Benzaldehyde with SiH_4 (B3LYP/6-311++G**)

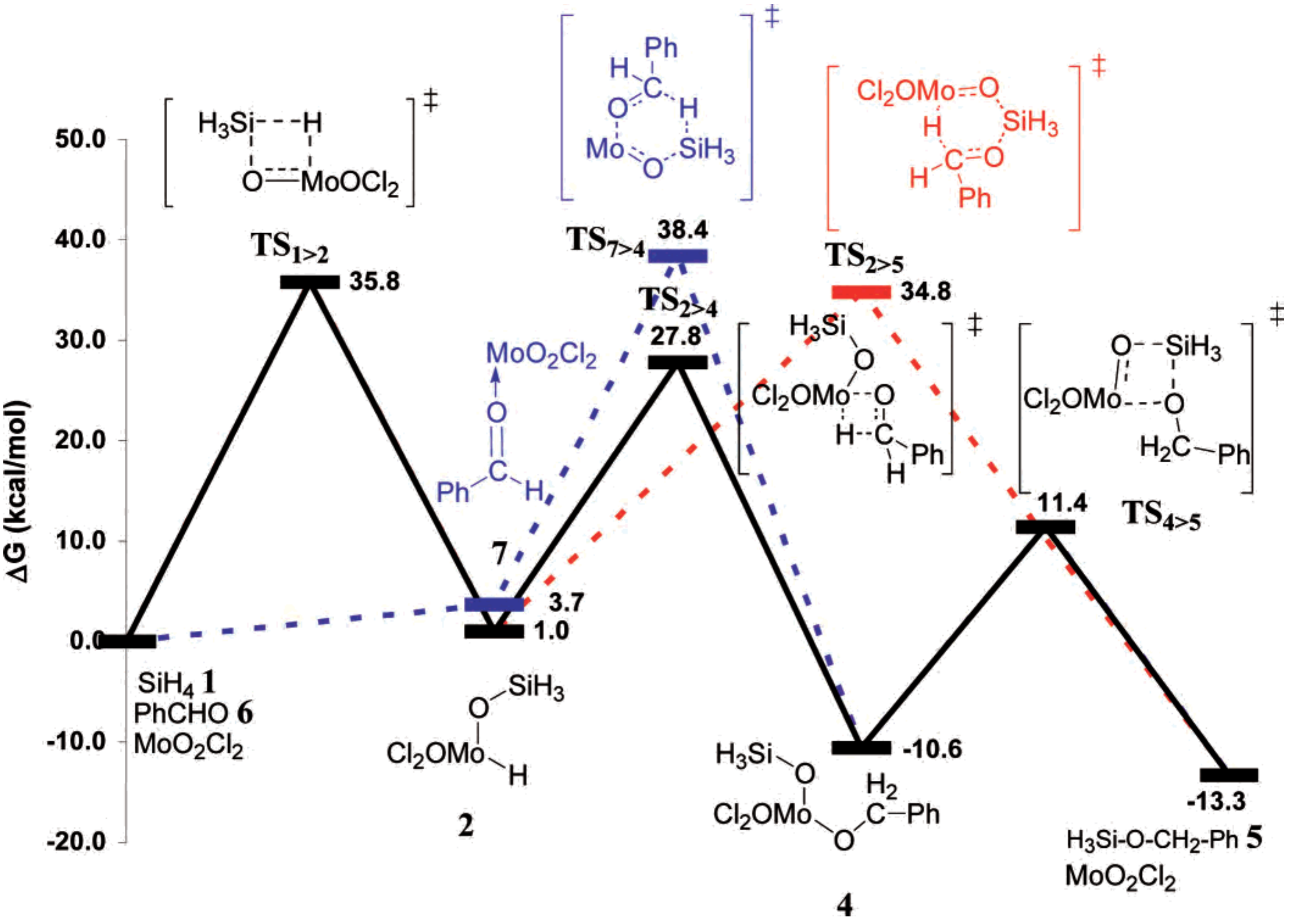

kcal/mol). Therefore, according to our DFT calculations, a reaction via intermediate **8** is highly improbable.

The reaction pathway starting by the initial activation of the carbonyl compound, which presumably could lead to the hydrosilylated product, is the sequence [starting materials (**1** and **6**) − adduct **7** (Figure 6) − $\mathbf{TS_{7>4}}$ − intermediate **4** − $\mathbf{TS_{4>5}}$ − product (**5**)]. The formation of **7** must have a very low barrier; no transition state could be calculated for the addition. The silane reacts with **7** via the cyclic transition state $\mathbf{TS_{7>4}}$ (Figure 6). The silyl group adds directly to MoO_2Cl_2, whereas the activated hydrogen is transferred to the carbonyl carbon C1, forming intermediate **4**, which is also part of the pathways starting with initial activation of the silyl compound and the hydrosilylation product via $\mathbf{TS_{4>5}}$ (Figure 3).

Comparing the free-energy barrier of $\mathbf{TS_{7>4}}$ (38.4 kcal/mol) to the highest barriers of the initial silane activation pathway, it is interesting to note that the reaction sequence [starting materials (**1** and **6**) − $\mathbf{TS_{1>2}}$ − **2** − $\mathbf{TS_{2>4}}$ − **4** − $\mathbf{TS_{4>5}}$ − product (**5**)] has the lower-rate determining-step ($\mathbf{TS_{1>2}}$, 35.8 kcal/mol). For the system MoO_2Cl_2/SiH_4/PhCHO, it can therefore be concluded that the catalytic hydrosilylation should start with the SiH activation via [2+2] cycloaddition at the catalyst, followed by carbonyl coordination to the metal center.

$PhMe_2SiH/MoO_2Cl_2 \Rightarrow C_6H_5CHO$

The silane, which (together with benzaldehyde) was used in the experiments by Romao et al.,[9] is a sterically more demanding compound ($PhMe_2SiH$). We calculated all of the pathways described above for this silane, but because most of the structures are comparable to the SiH_4 results, we decided to put them into the Supporting Information (we added an additional letter a to the numbers to differentiate the $PhMe_2SiH$ structures from the SiH_4 structures). In Scheme 5, free energies of the three most feasible pathways ($\mathbf{1a{-}TS_{1a>2a}{-}2a{-}TS_{2a>4a}{-}4a{-}TS_{4a>5a}{-}5a}$ / $\mathbf{1a{-}TS_{1a>2a}{-}2a{-}TS_{2a>5a}{-}5a}$ / $\mathbf{6{-}7{-}TS_{7>4a}{-}4a{-}TS_{4a>5a}{-}5a}$) for $PhMe_2SiH$ are shown. For comparison, the corresponding diagram for SiH_4 is given in Scheme 8.

According to Scheme 5, the most preferred pathway for $PhMe_2SiH$ should also be the initial silane activation, forming the hydride intermediate **2a**. Compared to the pathway via initial carbonyl activation ($\mathbf{TS_{7>4a}}$, 37.4 kcal/mol), the rate-determining step ($\mathbf{TS_{1a>2a}}$, 32.1 kcal/mol) is lower in energy. The differentiation of the barriers in the case of the sterically more demanding silane is significantly larger than that in the case of SiH_4 (cf. $\mathbf{TS_{1>2}}$ → 35.8 kcal/mol, $\mathbf{TS_{7>4}}$ → 38.2 kcal/mol). Considering the level of theory used the energy differences are significant and outside of the error limits of the method.

Our study is in good agreement with the results Wu et al.[21] have obtained for the hydrosilylation of $HSiMe_3$ and

Scheme 9. Proposed Catalytic Cycle According to Our DFT Calculations

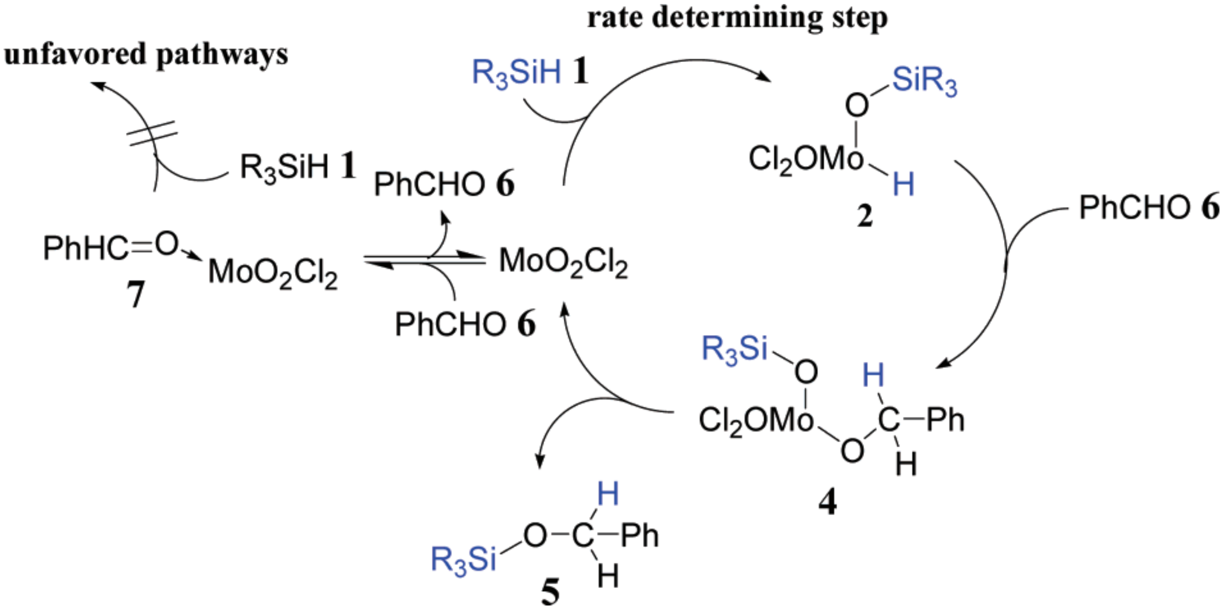

acetaldehyde in the presence of the dioxo compound $ReO_2I(PPh_3)_2$. They also favor initial silane activation via the [2+2] cycloaddition pathway. The corresponding [3+2] hydroxyl compound can be completely ruled out as the tautomerization has an even higher barrier than in the molybdenum case. The $Re(OTMS)OI(PPh_3)_2H$ intermediate reacts with the carbonyl compound via a stepwise addition and not by direct hydrosilylation via a cyclic transition state.

They also located transition states that are equivalent to $\mathbf{TS_{7>4}}$ for the initial carbonyl activation pathway and concluded that this barrier is too high in energy and that the rate-determining step is expected to be the initial silane activation. According to Wu et al., acetaldehyde could also undergo an oxygen exchange with the rhenium compound rather than a hydrosilylation after coordination to the metal. Their calculated barrier height of the same rate-determining step (initial [2+2] SiH activation) is on the same magnitude ($\Delta G^{\ddagger} = 37.7$ kcal/mol) as $\mathbf{TS_{1>2}}$ or $\mathbf{TS_{1a>2a}}$ shown above for the molybdenum catalyst. In contrast to the study on the double-ξ level of theory,[22] we can differentiate between the various pathways and are able to predict the pathway with clearly the lowest activation energies.

Conclusion

On the basis of triple-ξ DFT calculations, we propose that the catalytic hydrosilylation of benzaldehyde by MoO_2Cl_2 proceeds via initial silyl activation and a hydride intermediate. The aldehyde then adds to the metal center of the intermediate, followed by transfer of the hydrogen to the carbonyl carbon atom. Finally, the silyl group moves to the former carbonyl oxygen atom, separating from the catalyst MoO_2Cl_2 under the formation of the hydrosilylation product. The proposed catalytic cycle is shown in Scheme 9. All of the possible pathways via initial carbonyl activation are calculated to have larger barriers, although the formation of weakly bound **7** should be possible.

It is unusual that the metal-oxo compound MoO_2Cl_2 prefers to react via a [2+2] mechanism in the initial SiH activation step. Other metal-oxo compounds like permanganate, osmium tetraoxide, or ruthenium tetraoxide cleave a SiH bond much easier via a [3+2] pathway, similar to what we calculated for the activation of the CH bond. But the high exothermicity of the resulting intermediates prohibits a catalytic application of these metal-oxo compounds. Only in the case of the molybdenum compound MoO_2Cl_2, the thermoneutral hydride intermediate of the preferred [2+2] mechanism allows a catalytic reaction.

Acknowledgment. Financial support by the Fonds der Chemischen Industrie is gratefully acknowledged. The authors are especially grateful to the Center of High-Performance Computing (ZIH) of the Technische Universitaet Dresden for the computing time.

Supporting Information Available: Complete ref 25 and all of the *x*, *y*, *z* coordinates together with structures of the intermediates and transition states of the $PhMe_2SiH$ reaction. This material is available free of charge via the Internet at http://pubs.acs.org.

IC7017314